Journal of Constructional Steel Research 169 (2020) 106071

Contents lists available at ScienceDirect

Journal of Constructional Steel Research

Residual stresses of heat-treated and hot-dip galvanized RHS cold-formed by different methods

Kamran Tayyebi [a], Min Sun [a,*], Kian Karimi [b]

[a] Department of Civil Engineering, University of Victoria, Victoria, British Columbia V8P 5C2, Canada
[b] Department of Civil Engineering, British Columbia Institute of Technology, Vancouver, British Columbia V5G 3H2, Canada

ARTICLE INFO

Article history:
Received 26 February 2020
Received in revised form 30 March 2020
Accepted 1 April 2020
Available online xxxx

Keywords:
Galvanizing
Residual stress
Heat treatment
Rectangular hollow section
High-strength steel
Indirect-formed
Direct-formed

ABSTRACT

Rectangular hollow sections (RHS) are produced in diverse locations internationally to various specifications, predominantly by cold-forming. RHS cold-formed by different techniques have different material and residual stress properties. Hot-dip galvanizing and heat treatment are commonly applied post-cold-forming processes. A comprehensive literature review showed that dedicated research on the effects of these processes on the performances of tubular steel members and connections is insufficient. Also, there is no definitive published guidance on this topic from structural steel associations. In particular, further research on the effects of heat treatment at various temperatures for various durations is needed to ensure a fit-for-purpose process (e.g. improvement of compressive member behaviour) which consumes less energy. This paper reports a comprehensive experimental investigation on the residual stress properties of 26 RHS specimens with different grades (nominal yield strengths from 350 to 690 MPa), cold-formed by different techniques, and subsequently subjected to post-production galvanizing and heat treatments to different degrees.

1. Introduction

According to a complimentary literature review [1], to this day the implications of using Hollow Structural Section (HSS) materials manufactured by different techniques and subsequently subjected to different post-production processes are not fully appreciated. In particular, further research is needed on the effects of post-production hot-dip galvanizing and heat treatment to different degrees on HSS material [2,3]. This research covers Rectangular Hollow Sections (RHS) cold-formed by two predominant methods.

Hot-dip galvanizing is an efficient method for a reliable protection against corrosion that might affect the service lives of the steel structures. Due to the advantages in structural and economic aspects, galvanized trusses made of hollow sections are being increasingly used in exposed steel structures. Permanent or temporary building solutions are available for a wide range of sectors including aviation, industrial, marine, offshore, oil and gas, as well as sports (see Fig. 1 for examples). Based on experimental testing of a limited number of galvanized and ungalvanized hollow section members under axial compression [4–6], it was speculated that for cold-formed HSS, the hot-dip galvanizing process may sometimes effectively reduce the overall level of residual stress contained in the cross section, similar to a heat treatment process described in ASTM A1085 Supplement S1 [7] and CSA G40.20/G40.21 [8]. It should be noted that the intention of the latter is to partially relieve the residual stresses in steel members to improve the compressive member behaviours. This type of heat treatment is typically conducted at a temperature of 450 °C or higher for a 30-min holding time, followed by cooling in air. On the other hand, the hot-dipping process of steel members (of commonly specified sizes) in a molten zinc bath (typically maintained at a temperature of 450 °C) only takes approximately 10 min [1,2]. Hence, the fit-for-purpose heat treatment duration (for a partial release of residual stress and improvement of compressive member behaviour) needs to be revisited, via a comprehensive residual stress measurement on hollow sections with different production histories.

In North America, RHS materials are predominantly cold-formed by two methods: indirect-forming and direct-forming. RHS materials produced by the two methods can have the same appearances but very different structural behaviours [6]. This research covers North American-produced RHS with different grades and cold-formed by the two predominant methods in order to develop general conclusions on the effects of different post-cold-forming processes. In particular, a new type of high-strength RHS product cold-formed by the direct-forming approach is included in this research. The new material has a nominal yield strength of 690 MPa. Recent research showed that the new RHS material has superior stub column behaviour, comparing to the conventional RHS [6]. In addition, the cross section classification rules in North American steel design standards for elements under

* Corresponding author.
E-mail address: msun@uvic.ca (M. Sun).

https://doi.org/10.1016/j.jcsr.2020.106071
0143-974X/

(a) Aviation (b) Sports

(c) Transportation (d) Parking

Fig. 1. Galvanized tubular steel structures.

axial compression were proven to be unnecessarily conservative for the new RHS product. It was speculated that the superior behaviour was due to an inherently low level of residual stress as a result of the unique manufacturing approach, where the cold-forming is only concentrated at the four corner regions. Since research on direct-formed high-strength RHS is still limited, with the aim of generating design tools to facilitate the application of the new construction material in North America, special attention is given to it in this research. The residual stresses in RHS of similar cross-sectional dimensions with regular strength (nominal yield strength = 350 MPa) and cold-formed by both the direct-forming method and the indirect-forming method were also measured for comparison.

2. Background

2.1. Galvanizing

The galvanizing process starts with surface preparation (degreasing, pickling, and further cleaning using a flux solution) to ensure a proper chemical reaction between the molten zinc bath and the steel during hot-dipping. The molten zinc bath is typically maintained at a temperature of approximately 450 °C. The final hot-dipping process during galvanizing of steel members of commonly specified sizes only takes approximately 10 min [1,2]. In order to control the reactivity between steel and molten zinc mixture, no significant change can be made to bath temperature or dipping time. Recent research has been performed on the effects of general galvanizing practice and structural details on: (1) the possible changes in material properties, and (2) the thermally-induced stress and strain demands on structural components. Critical reviews of the relevant research can be found in [2,3]. The hot dipping process in general does not change the steel microstructure and grain size. However, the residual stresses in cold-formed steels can be reduced [2,3].

For hot-dip galvanizing of welded tubular steel trusses and girders, holes to allow for filling, venting and drainage must be specified at the welded joint location of the connections. Adequate sizing of the galvanizing holes also minimizes the differential thermal stresses experienced by the structure during the hot-dipping process. Detailed discussions on the effect of such holes on the connection behaviours under static and fatigue loadings can be found in [9–11].

2.2. Heat treatment

In North America, two steel product standards, ASTM A1085 [7] and CSA G40.20/40.21 [8], contain heat treatment rules for justification of an improved compressive member behaviour for an HSS member (e.g. the use of a high column curve in the Canadian steel design standard CSA S16–19 [12]). Both ASTM A1085 [7] and CSA G40.20/40.21 [8] specify a furnace temperature of 450 °C or higher for such process (see Fig. 2 for an example). However, neither manufacturing standard specifies the holding time or total duration. Since there is no definitive requirement, in practice heat treaters generally hold the furnace temperature at 450 °C for 30 min [1–3]. Previous research by Sun and Packer [13] found that such heat treatment has negligible effect on the Charpy

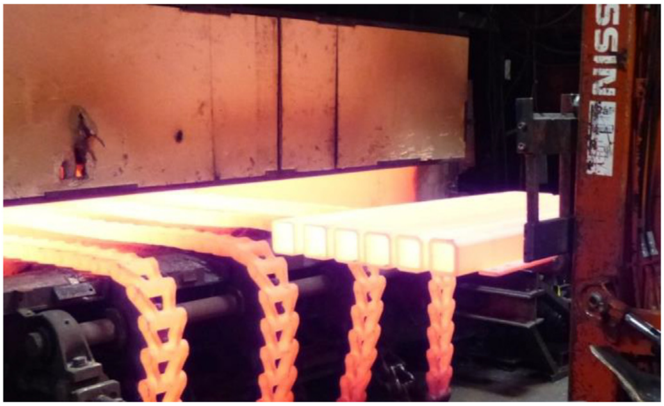

Fig. 2. Removal of RHS material from furnace.

V-notch impact toughness of cold-formed RHS material, since it does not change the steel microstructure or grain size. Recently, via a comprehensive experimental research on RHS stub columns, Tayyebi and Sun [6] found that the hot-dip galvanizing process can also effectively improve the structural performance of cold-formed RHS under axial compression. Similar observations have been made in the investigations on galvanized CHS column members by Shi et al. [4,5]. Hence, one can deduce that for the 450 °C post-production heat treatment per [7,8] for improvement of column behaviour, a 30-min holding time is likely excessive. However, research evidence is needed to support this speculation. Therefore, this investigation measures the residual stresses in galvanized and heat-treated hollow sections cold-formed by different methods. The aim is to find a fit-for-purpose duration for such heat treatment such that it consumes less energy. Another occasionally applied post-production heat treatment option at a temperature of 595 °C or higher is available with ASTM A143 [14]. The main objective of the 595 °C heat treatment is to further reduce residual stress, and to recover the loss of material ductility due to severe cold deformation such as cold-bending and roll-forming. This type of heat treatment is also included in the test matrix of this study for comparison.

2.3. Cold-forming methods

In North America, RHS of commonly specified cross-sectional dimensions are cold-formed by either direct-forming or indirect-forming. For the direct-forming method, flat rollers (see Fig. 3(a)) are used to form the coil strip directly into the desired rectangular cross section (see Fig. 3(b)). For the indirect-forming method, the coil strip is first cold-shaped into a circular form using concave rollers (see Fig. 3(c)). The circular shape is then further flattened into the desired rectangular shape, as shown in Fig. 3(d). Intuitively one can deduce that the residual stress magnitude in an indirect-formed RHS will be higher comparing to that in its direct-formed counterpart. One can also expect that the increase of yield strength from flat face to corner of a direct-formed RHS will be larger than that of its indirect-formed RHS counterpart, since during the direct-forming process, only the corner regions of the cross section are heavily cold worked (i.e. strain hardened). On the other hand, the level of cold working around the cross section is relatively uniform during the indirect-forming process.

Also associated with cold forming is the generation of residual stresses. Longitudinal residual stress is important for structural stability research. Compression members with high longitudinal residual stress levels are likely to experience early yielding. One can see the significance of longitudinal residual stresses over a cross section by superimposing the applied stress on them. As the loading increases, the summation of the applied and residual stresses causes some portions of the cross section to yield before others, which in return leads to a reduction in stiffness and in turn a loss in load-carrying capacity [6]. A good understanding of transverse residual stresses at corner regions of severely cold-formed RHS members is important for prevention of cracking during hot-dip galvanizing. Experience has shown that when cracking occurs during galvanizing, it usually initiates at the corner regions of the RHS free end. The RHS free end tends to "open" during galvanizing as a result of high residual and thermal stresses in the transverse direction. The risk of cracking can be reduced by welding end plates to the RHS to restrain the expansion of the section [1–3].

In all, although extensive research on the material properties of hollow sections [15–33], the difference among cold-formed, galvanized, lightly heat-treated (at 450 °C), and heavily heat-treated (at 595 °C) hollow sections has been a point of debate to date [1,2]. This paper focuses on their residual stress properties.

3. Preparation of RHS specimens

3.1. Parent hollow sections

Eleven parent tubes made of steels with different grades and produced by the two predominant cold-forming approaches were used to fabricate a total of 26 RHS specimens in this research. Each parent RHS ID in Table 1 contains two components. The first differentiates the material by its nominal yield strength ($\sigma_{y,nom}$) and cold-forming process, where I = regular-strength indirect-formed material ($\sigma_{y,nom}$ = 350 MPa); D = regular-strength direct-formed material ($\sigma_{y,nom}$ = 350 MPa); and DH = high-strength direct-formed material ($\sigma_{y,nom}$ = 690 MPa). The nominal external width, external height and wall thickness (in mm) are used in the second component of the parent RHS ID. The regular-strength materials (D and I) were produced to Gr. 350 W Class C of CSA G40.20/40.21 [8]. The high-strength materials (DH) were produced to ASTM A1112 Gr. 100 [34]. All direct-formed materials (D and DH) were cold-formed in the same production facility to allow direct comparison and to study individually the effects of different material strengths. The selection of specimens also allows the direct comparisons of residual stresses in RHS over a wide range of cross-sectional dimensions. Prior to tests, the cross-sectional dimensions were carefully measured and are listed in Table 1. Table 2 shows the chemical compositions of the parent RHS.

3.2. Post-cold-forming heat treatment and galvanizing

This research sought to: (1) determine the fit-for-purpose duration and temperature for heat treatment to improve compressive member behaviour of cold-formed RHS; and (2) quantify the effects of hot-dip galvanizing on residual stress properties of cold-formed RHS. Hence, using the 11 parent hollow sections, 26 RHS specimens of different production histories were prepared and are listed in Table 1. As shown, a third component was added to the specimen ID, to differentiate the materials by the post-production processes they received. For the third ID component, "U" and "G" represent as-received untreated and galvanized cold-formed RHS, respectively. Neither was subjected to post-cold-forming heat treatment. "450" and "595" represent RHS heat-treated to 450 °C per [7,8] and 595 °C per [14], respectively. Similar furnace cycles were applied to all heat-treated specimens (i.e. hold the specified furnace temperature for 30 min) for the purpose of direct comparison. As discussed in Section 2.2, the furnace cycles are consistent with the current industrial practice.

4. Tensile coupon test

4.1. Test procedures

For all 26 RHS specimens, the material properties were determined via tensile coupon tests following the requirements in ASTM E8 [35]. The tensile coupons were cut from the flat faces and the corners of the

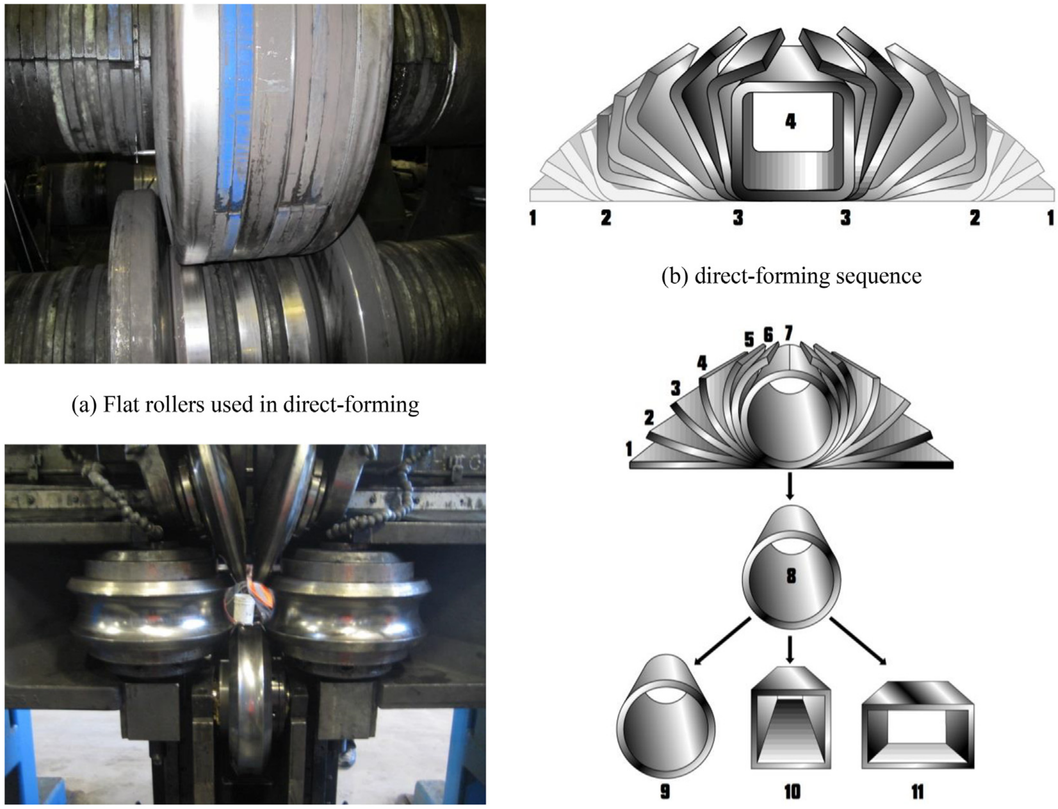

(a) Flat rollers used in direct-forming

(b) direct-forming sequence

(c) Concave rollers used in indirect-forming

(d) indirect-forming sequence

Fig. 3. Different cold-forming approaches.

Table 1
Measured dimensions of parent RHS.

Parent RHS ID	B (mm)	H (mm)	t (mm)	r_{i1} (mm)	r_{i2} (mm)	r_{i3} (mm)	r_{i4} (mm)	RHS specimen ID
I-102 × 102 × 6.4	102.1	102.2	6.41	7.2	6.6	8.9	9.1	I -102 × 102 × 6.4- U I -102 × 102 × 6.4–450 I -102 × 102 × 6.4–595 I -102 × 102 × 6.4- G
I-102 × 102 × 7.9	101.9	102.1	7.83	11.0	11.9	13.0	10.8	I -102 × 102 × 7.9- U I -102 × 102 × 7.9–450 I -102 × 102 × 7.9–595 I -102 × 102 × 7.9- G
I-102 × 102 × 13	101.6	101.7	12.90	11.8	11.6	11.7	11.9	I -102 × 102 × 13- U I -102 × 102 × 13–450 I -102 × 102 × 13–595 I -102 × 102 × 13- G
D − 76 × 102 × 3.2	76.5	101.9	3.03	2.6	2.8	2.1	2.0	D - 76 × 102 × 3.2- U D - 76 × 102 × 3.2- G
D-76 × 102 × 4.8	76.4	101.9	4.36	2.5	3.4	3.7	4.2	D - 76 × 102 × 4.8- U D - 76 × 102 × 4.8- G
D-102 × 102 × 4.8	101.6	102.1	4.40	5.6	5.4	4.5	7.1	D - 102 × 102 × 4.8- U
DH-76 × 76 × 4.8	76.3	76.6	4.81	10.2	7.7	8.7	7.3	DH -76 × 76 × 4.8- U DH -76 × 76 × 4.8- G
DH-76 × 102 × 3.2	76.9	102.6	3.02	2.2	2.7	2.9	2.6	DH -76 × 102 × 3.2- U DH -76 × 102 × 3.2- G
DH-76 × 102 × 4.1	76.3	101.8	4.06	5.2	5.6	3.9	4.3	DH -76 × 102 × 4.1- U
DH-76 × 102 × 4.8	76.6	102.0	4.82	9.2	9.2	8.5	8.5	DH -76 × 102 × 4.8- U DH -76 × 102 × 4.8- G
DH-76 × 152 × 4.1	77.2	153.1	4.04	6.3	4.4	5.0	4.6	DH -76 × 152 × 4.1- U DH -76 × 152 × 4.1- G

Table 2
Chemical compositions of parent RHS.

Parent RHS ID	C	Si	Mn	Cu	Ni	Cr	Mo	V	Ti	CE
I-102 × 102 × 6.4	0.140	0.240	0.870	0.010	0.050	0.003	0.000	0.003	N/A	0.29
I-102 × 102 × 7.9	0.140	0.230	0.860	0.010	0.050	0.040	0.000	0.013	N/A	0.30
I-102 × 102 × 13	0.200	0.023	0.750	0.020	0.008	0.026	0.002	0.002	0.002	0.33
D-76 × 102 × 3.2	0.180	0.020	0.390	0.140	0.060	0.080	0.020	0.001	0.001	0.28
D-76 × 102 × 4.8	0.040	0.040	0.710	0.120	0.040	0.060	0.000	0.002	0.000	0.18
D-102 × 102 × 4.8	0.061	0.029	0.610	0.014	0.010	0.020	0.002	0.001	0.002	0.17
DH-76 × 76 × 4.8	0.061	0.020	1.650	0.010	0.030	0.030	0.000	0.010	0.000	0.35
DH-76 × 102 × 3.2	0.072	0.020	1.350	0.010	0.040	0.020	0.000	0.010	0.120	0.31
DH-76 × 102 × 4.1	0.078	0.020	1.340	0.010	0.030	0.030	0.000	0.010	0.110	0.31
DH-76 × 102 × 4.8	0.061	0.020	1.690	0.010	0.030	0.020	0.000	0.010	0.080	0.35
DH-76 × 152 × 4.1	0.080	0.020	1.330	0.010	0.040	0.030	0.010	0.010	0.110	0.32
Cast analysis (%)										
Note: carbon equivalent	$CE = C + \frac{Mn}{6} + \frac{Cr + Mo + V}{5} + \frac{Ni + Cu}{15}$									

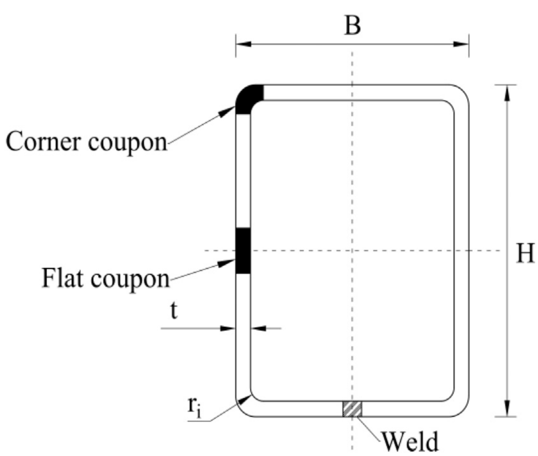

Fig. 4. Locations of tensile coupons.

cross sections (see Fig. 4). An extensometer and a pair of strain gauges were installed on the coupon to determine the strains. Representative stress-strain curves are shown in Figs. 5 to 8. Tables 3 and 4 list the key tensile coupon test results.

4.2. Discussions of tensile coupon test results

4.2.1. Effects of cold-forming methods

Using the data in Tables 3 and 4, for the untreated specimens (i.e. 3rd ID component = U), the changes of yield strength, ultimate strength and rupture strain from the flat face to the corner region of the cross sections are shown in Fig. 9. As discussed in Section 2.3, for direct-formed RHS, only the corner regions are heavily cold worked, while for the indirect-formed RHS, the entire cross section is heavily cold worked. According to Fig. 9(a), the yield strength increases from flat face to corner of the direct-formed RHS (D and DH) are larger than those of the indirect-formed RHS (I), which is consistent with the speculations based on the comparison between the two cold-forming approaches. For the three indirect-formed RHS, the increase in yield strength decreases as the wall thickness increases, since the degree of cold working over the perimeter of the cross section becomes more uniform as the width-to-thickness ratio increases. Similar observations can be made in Fig. 9(b) for the ultimate strength. Since steel producers often aim at rolling RHS with large "flat width" dimensions, the overall amount of cold working and in turn the residual stress level in the cross section

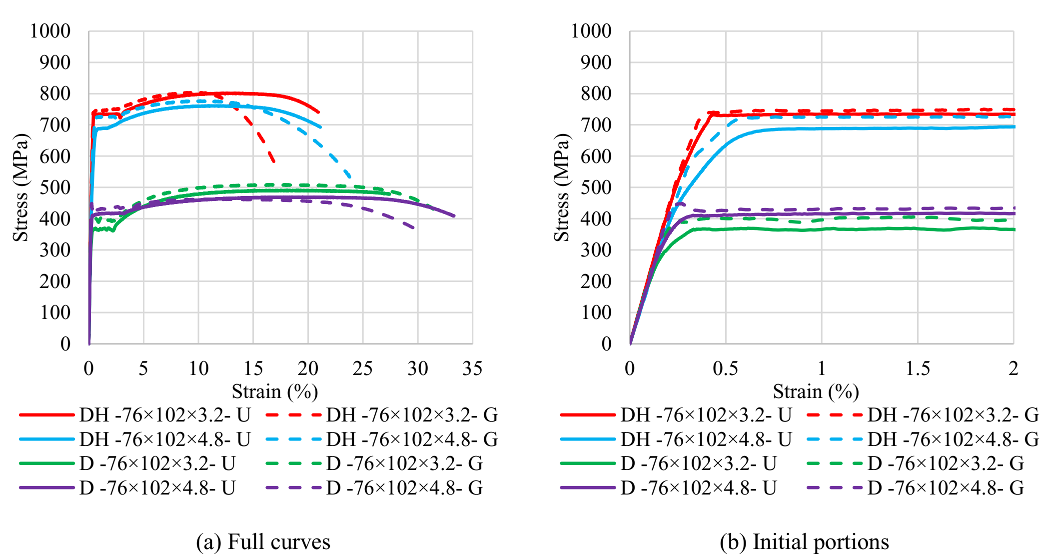

Fig. 5. Representative tensile stress-strain relationships of flat coupons from direct-formed RHS.

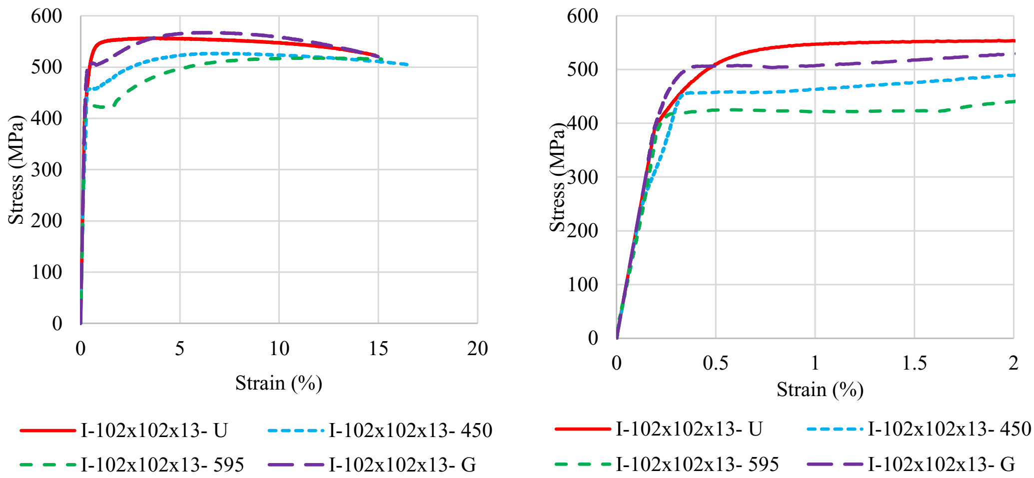

(a) Full curves (b) Initial portions

Fig. 6. Representative tensile stress-strain relationships of flat coupons from indirect-formed RHS.

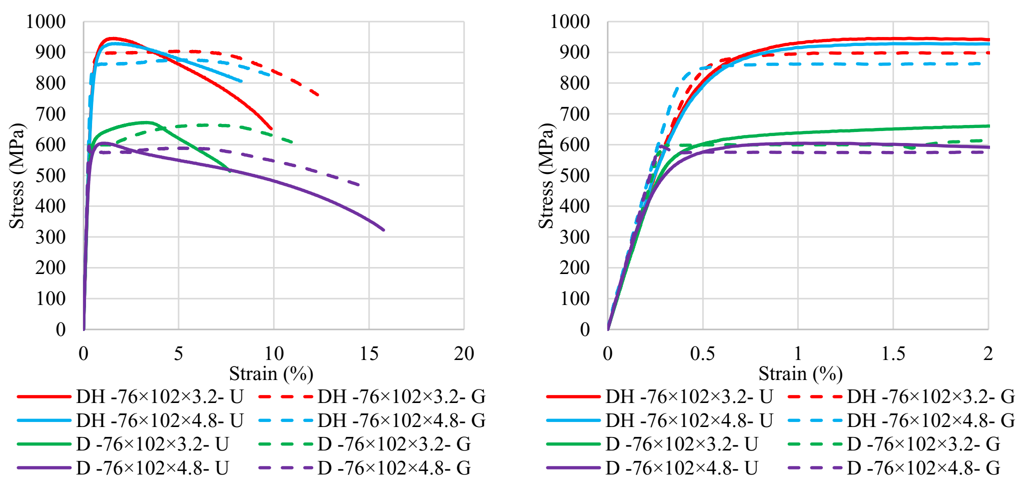

(a) Full curves (b) Initial portions

Fig. 7. Representative tensile stress-strain relationships of corner coupons from direct-formed RHS.

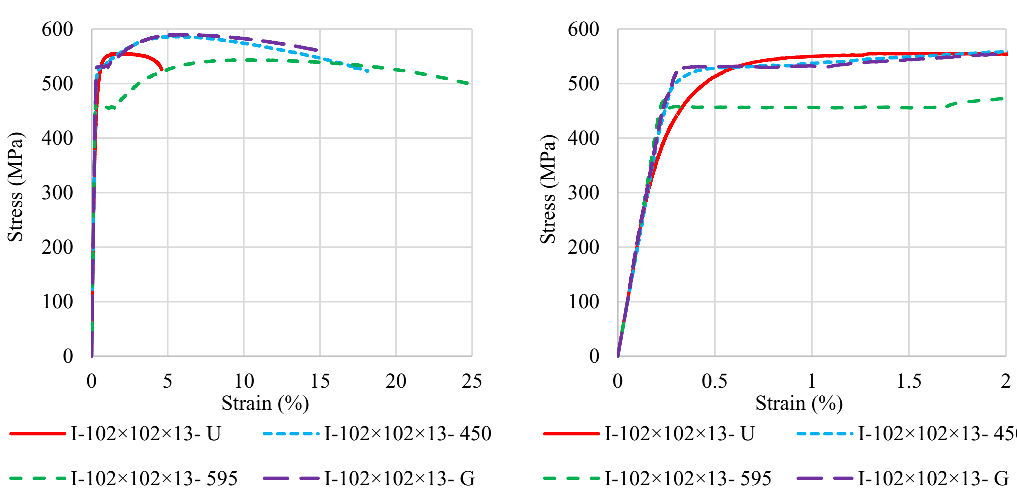

(a) Full curves (b) Initial portions

Fig. 8. Representative tensile stress-strain relationships of corner coupons from indirect-formed RHS.

Table 3
Flat coupon test results.

Specimen ID	E (GPa)	σ_y (MPa)	σ_u (MPa)	ε_u (%)	ε_r (%)	σ_u/σ_y	$\varepsilon_u/(\sigma_y/E)$
I-102 × 102 × 6.4-U	199	415	482	16.0	30	1.16	76.7
I-102 × 102 × 6.4–450	201	427	505	12.5	31	1.18	58.8
I-102 × 102 × 6.4–595	200	384	486	15.2	33	1.27	79.2
I-102 × 102 × 6.4-G	203	445	509	10.1	27	1.14	46.1
I-102 × 102 × 7.9-U	198	458	509	9.5	25	1.11	41.1
I-102 × 102 × 7.9–450	208	468	539	8.6	26	1.15	38.2
I-102 × 102 × 7.9–595	206	409	505	13	31	1.23	65.5
I-102 × 102 × 7.9-G	194	478	530	6.8	22	1.11	27.6
I-102 × 102 × 13-U	201	483	549	4.4	22	1.14	18.3
I-102 × 102 × 13–450	201	480	566	5.6	25	1.18	23.5
I-102 × 102 × 13–595	196	433	527	10.5	30	1.22	47.5
I-102 × 102 × 13-G	207	493	555	6.3	25	1.13	26.5
D-76 × 102 × 3.2-U	203	367	492	15.1	34	1.34	83.5
D-76 × 102 × 3.2-G	211	400	509	17.3	32	1.27	91.3
D-76 × 102 × 4.8-U	200	409	470	19.5	39	1.15	95.4
D-76 × 102 × 4.8-G	204	424	463	10.3	36	1.09	49.6
D-102 × 102 × 4.8-U	205	399	487	12.9	38	1.22	66.3
DH-76 × 76 × 4.8-U	199	638	767	10	27	1.20	31.2
DH-76 × 76 × 4.8-G	203	743	786	9.8	28	1.06	26.8
DH-76 × 102 × 3.2-U	217	730	802	12.6	27	1.10	37.5
DH-76 × 102 × 3.2-G	217	742	803	9.3	20	1.08	27.2
DH-76 × 102 × 4.1-U	202	692	776	11.8	26	1.12	34.4
DH-76 × 102 × 4.8-U	194	651	761	10.9	29	1.17	32.5
DH-76 × 102 × 4.8-G	191	720	777	9.5	26	1.08	25.2
DH-76 × 152 × 4.1-U	198	713	815	13.9	30	1.14	38.6
DH-76 × 152 × 4.1-G	208	744	819	12.1	28	1.10	33.8

of an indirect-formed RHS should in theory be much higher than that in its direct-formed counterpart. This speculation is substantiated in Section 5.

4.2.2. Effects of galvanizing and heat treatment

Using the data in Tables 3 and 4, the effects of the 450 °C heat treatment, the 595 °C heat treatment and the hot-dip galvanizing process on the material yield and ultimate strengths are compared in Fig. 10. As shown, both the 450 °C heat treatment per [7,8] and galvanizing had minor effect on the strength properties of materials from different locations of the cross sections. On the other hand, the 595 °C heat treatment per ASTM A143 [14] led to significant reduction in yield strength, and in some cases significant reduction in ultimate strength.

In both EN 1993-1-1:2005 [36] and EN 1993-1-12:2007 [37], the minimum ductility required for design is expressed in terms of limits for: (1) the ratio of the specified minimum tensile strength to the specified minim yield strength; (2) the rupture strain at the test region of a tensile coupon; and (3) the ratio of the ultimate strain to the yield strain of a tensile coupon. The requirements are listed in Table 5.

In AISC 360–16 [38] the minimum ductility required for design is expressed in a similar manner. Structural steel material conforming to one of the listed ASTM or CSA standards is approved for use under

Table 4
Corner coupon test results.

Specimen ID	E (GPa)	σ_y (MPa)	σ_u (MPa)	ε_u (%)	ε_r (%)	σ_u/σ_y	$\varepsilon_u/(\sigma_y/E)$
I-102 × 102 × 6.4-U	198	496	544	1.4	14	1.10	5.6
I-102 × 102 × 6.4–450	199	550	610	6.7	21	1.11	24.2
I-102 × 102 × 6.4–595	198	434	502	9.8	26	1.16	44.7
I-102 × 102 × 6.4-G	200	508	554	4.8	16	1.09	18.9
I-102 × 102 × 7.9-U	201	539	577	1.3	14	1.07	4.8
I-102 × 102 × 7.9–450	205	566	629	6.3	21	1.11	22.8
I-102 × 102 × 7.9–595	202	485	559	9.0	25	1.15	37.5
I-102 × 102 × 7.9-G	201	539	590	5.6	17	1.09	20.9
I-102 × 102 × 13-U	198	506	563	1.6	14	1.11	6.3
I-102 × 102 × 13–450	201	528	592	5.3	19	1.12	20.2
I-102 × 102 × 13–595	204	459	546	9.7	26	1.19	43.1
I-102 × 102 × 13-G	206	538	596	5.8	17	1.11	22.2
D-76 × 102 × 3.2-U	200	601	672	3.3	14	1.12	11.0
D-76 × 102 × 3.2-G	208	599	664	6.4	16	1.11	22.2
D-76 × 102 × 4.8-U	217	568	605	1.1	18	1.07	4.2
D-76 × 102 × 4.8-G	225	574	595	4.6	20	1.04	18.0
D-102 × 102 × 4.8-U	206	574	618	1.2	18	1.08	4.3
DH-76 × 76 × 4.8-U	190	789	863	1.4	19	1.09	3.4
DH-76 × 76 × 4.8-G	229	878	893	5.6	22	1.02	14.6
DH-76 × 102 × 3.2-U	206	862	945	1.6	12	1.10	3.8
DH-76 × 102 × 3.2-G	207	876	904	5.1	14	1.03	12.1
DH-76 × 102 × 4.1-U	211	879	960	1.3	12	1.09	3.1
DH-76 × 102 × 4.8-U	206	849	928	1.8	16	1.09	4.4
DH-76 × 102 × 4.8-G	225	816	876	5.3	20	1.07	14.6
DH-76 × 152 × 4.1-U	204	930	1054	1.8	14	1.13	3.9
DH-76 × 152 × 4.1-G	222	918	949	5.2	16	1.03	12.6

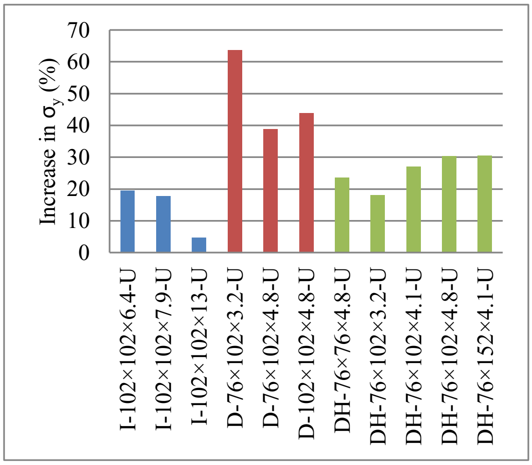

(a) Increase of yield strength

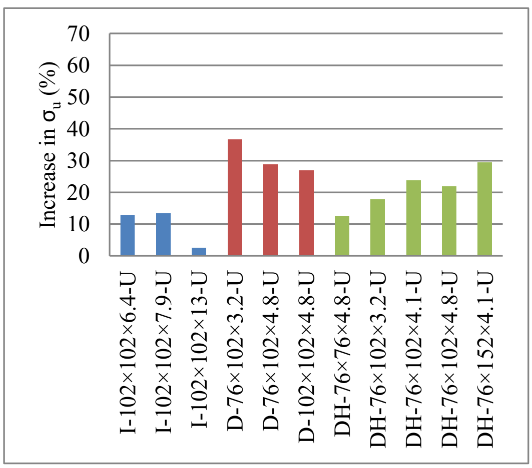

(b) Increase of ultimate strength

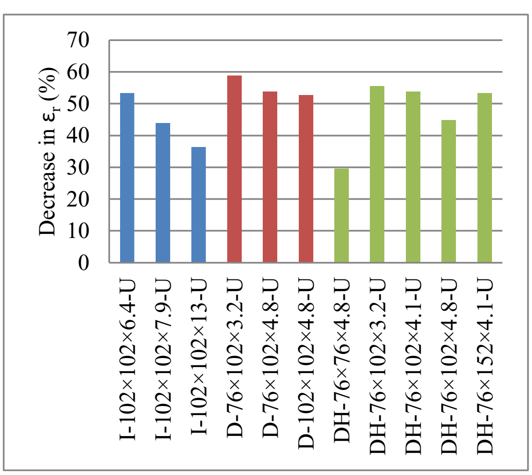

(c) Decrease of rupture strain

Fig. 9. Changes of material properties from flat face to corner region.

AISC 360–16. For cold-formed HSS, ASTM A500 [39], ASTM A1085 [7], and CSA-G40.20/G40.21 [8] are included in AISC 360–16 [38]. The minimum ductility in these steel product standards are similar to those in Eurocode 3 [36,37] and are shown in Table 6. As discussed in Section 3.1, the high-strength materials (DH) in this research were produced to ASTM A1112 Gr. 100 [34]. The ductility requirements from ASTM A1112 are also listed in Table 6.

Using the same criteria in the above standards and the data in Tables 3 and 4, the effects of galvanizing and heat treatments to different degrees on the material ductility (expressed in terms of the measured values of ε_r and σ_u /σ_y) are shown in Fig. 11. As shown, both galvanizing and heat treatment at 450 °C per [7,8] had minor effect on the ductility of the flat and corner coupons. On the other hand, the 595 °C heat treatment per ASTM A143 [14] led to significant reduction material ductility. However, the trade-off between ductility and strength must be taken in to consideration by the designers and fabricators when specifying the ASTM A143 [14] heat treatment.

5. Residual stress measurement

In this research, the sectioning technique recommended by the Structural Stability Research Council (SSRC) [40] was applied to measure the residual stresses in the longitudinal direction. A total of 342 strips were carefully machined from the 26 RHS specimens. Following the same approach used by [5,41–44], mechanical gauges were used to measure strip deformations for calculation of the in-situ residual stresses. A typical test piece (D-76 × 102 × 4.8-U) is illustrated in Fig. 12. Following the requirements in the SSRC guide [40], all test pieces were cut from a location at least three times the largest cross-sectional dimension away from the ends of the parent tubes. The width of each strip was 10 mm. Through-thickness gauge holes were drilled prior to sectioning. For each RHS test piece, after measuring the initial distances between the gauge holes, the cross section was cut open using a horizontal band saw. The sectioning setup is shown in Fig. 13. Liquid coolant was used throughout the process to minimize the heat input from cutting. After cutting, all strips were cooled to ambient temperature before measurements of the final distances between the gauge holes. Both the initial and the final gauge length measurements were repeated three times, and the average values were used in the residual stress calculations.

Before calculation, the deformed shapes of the strips from RHS with different production histories were compared. The deformed strips from typical RHS are shown in Figs. 14 and 15. In general, the strips from the untreated test pieces (Figs. 14(a), 15(a) and (c)) were heavily deformed. The deformations of the strips from RHS subjected to galvanizing (Figs. 14(b), (b) and (d)) and heat treatment at 450 °C for a holding time of 30 min (Fig. 14(c)) are similar and a lot smaller. This very clearly indicated similar amounts of reduction in residual stress from the two very different post-production processes. It should be noted that the 450 °C heat treatment in this case is much more onerous comparing to hot-dip galvanizing, as discussed in Section 2.2. The heat treatment at 595 °C for a holding time of 30 min released almost all residual stresses since the strips remained straight after sectioning (Fig. 14(d)).

5.1. Calculation of residual stresses

For measurement of the relaxation of strains resulting from removal of material, this research applied the standard procedures and the standard mechanical gauges recommended by the SSRC guide [35]. The same approach has been used in previous research on cold-formed steel members [5,36–38]. As illustrated in Fig. 16, the sectioning method in the SSRC guide [35] assumes a linear though-thickness distribution of residual stress, which can be determined by measuring the elastic spring back upon removal of strips from the cross section. In Fig. 16, σ_{in} and σ_{out} are the total longitudinal residual stresses on the inside and outside surfaces of the strip, respectively. The membrane residual stress (σ_m) is the mean of σ_{in} and σ_{out}. The bending residual stress (σ_b) is the deviation of the total from the membrane component. A Whittemore gauge with an accuracy of 0.00254 mm over a gauge length of 254 mm was employed to measure the change in length of the strips (axial deformations). The bending deformation of each strip was

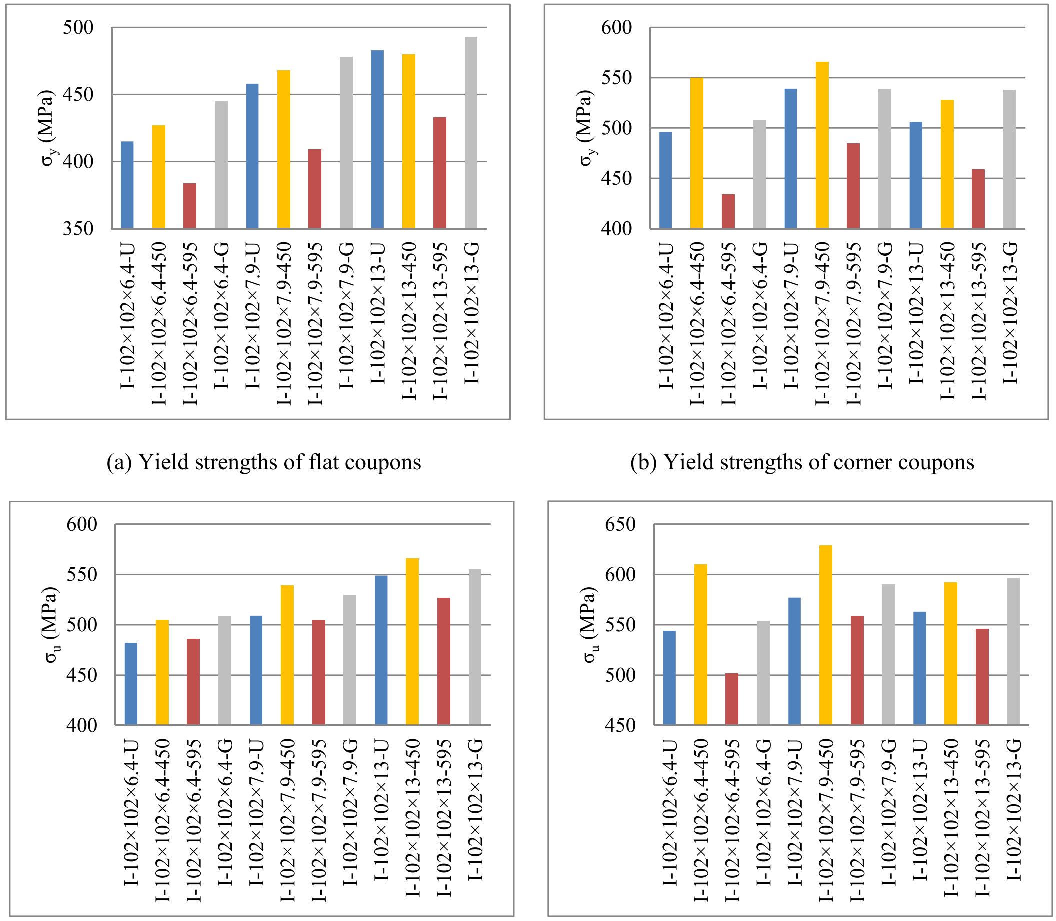

(a) Yield strengths of flat coupons

(b) Yield strengths of corner coupons

(c) Ultimate strengths of flat coupons

(d) Ultimate strengths of corner coupons

Fig. 10. Yield and ultimate strengths of RHS materials subjected to different post-cold-forming processes.

Table 5
Ductility requirement in Eurocode 3.

EN 1993-1-1:2005 [36]	EN 1993-1-12:2007 [37]
$\sigma_u / \sigma_y \geq 1.10$ $\varepsilon_r \geq 15\%$ $\varepsilon_u / (\sigma_y / E) \geq 15$	$\sigma_u / \sigma_y \geq 1.05$ $\varepsilon_r \geq 10\%$ $\varepsilon_u / (\sigma_y / E) \geq 15$

determined by measuring the deflections at various locations by using a Mitutoyo digital height gauge with an accuracy of 0.01 mm. Since all measurements were performed in a lab space (with temperature control), the effect of temperature change on the readings was considered negligible. The bending and membrane residual stresses were calculated by applying the same procedures used by Gardner and Cruise [44] as well as Yuan et al. [42].

5.2. Discussions of residual stress measurement results

The membrane and bending residual stress distributions in the longitudinal direction of the 26 RHS specimens are shown in Figs. 17 and 18, respectively. In these figures, the residuals stresses at the flat face and corner regions are normalized by the measured yield stress (σ_y) of tensile coupon at the corresponding location. The start and end points in Figs. 17 and 18 are consistent with Fig. 12. In Figs. 17 and 18, compressive residual stresses are shown as negative values and tensile residual stresses as positive values. Fig. 18 shows only the bending residual stresses on the external surfaces of the RHS specimens. The averages of the normalized values for different regions over the cross sections are listed in Table 7. The overall cross-sectional values in Table 7 are calculated using a weighted average method (i.e. residual stress × tributary area in Fig. 12 / total cross-sectional area). The overall cross-sectional values are especially useful for comparison of residual stresses

Table 6
Ductility requirements in ASTM and CSA standards approved for use under AISC 360–16.

Standard	Grade	Minimum specified ε_r (%)	Minimum specified σ_y (MPa)	Minimum specified σ_u (MPa)	σ_u / σ_y
ASTM A500 [39]	C	21	345	425	1.23
ASTM A1085 [7]	A	21	345	450	1.30
CSA-G40.20/G40.21 [8]	350 W	22	350	450	1.29
ASTM A1112 [34]	100	12	690	760	1.10

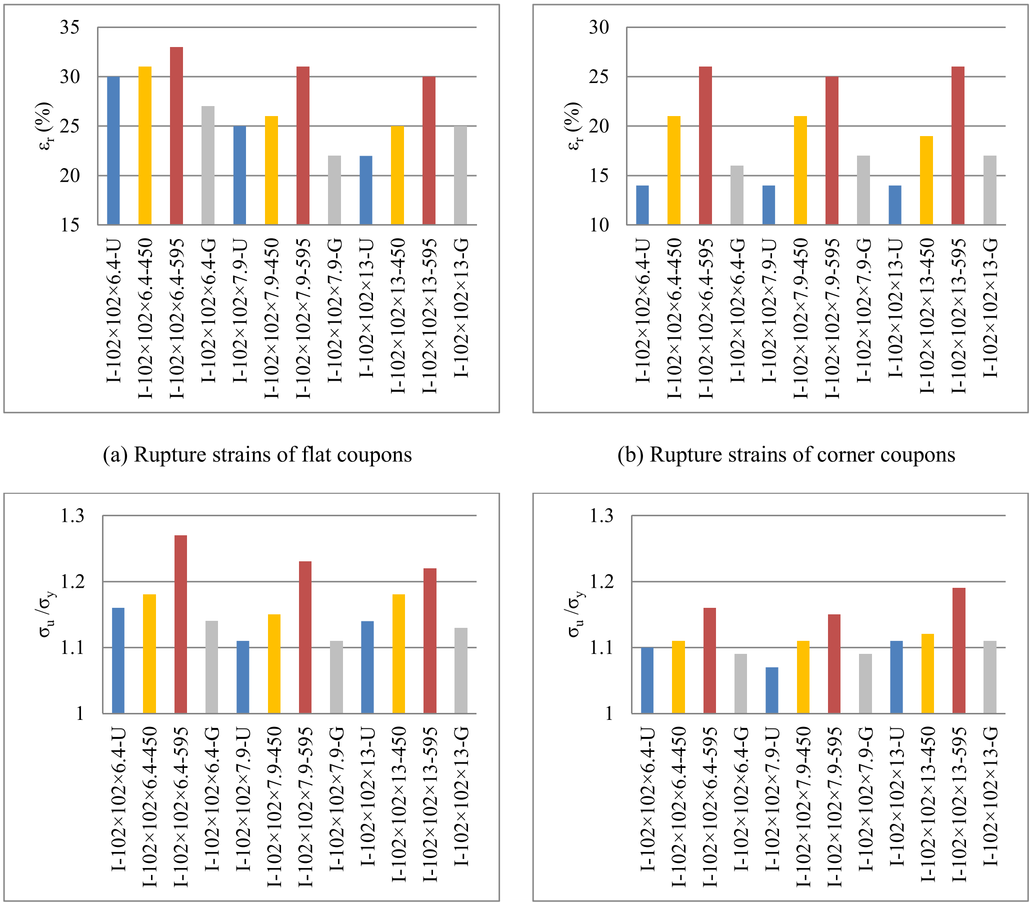

(a) Rupture strains of flat coupons

(b) Rupture strains of corner coupons

(c) σ_u /σ_y-values of flat coupons

(d) σ_u /σ_y-values of corner coupons

Fig. 11. Ductility of RHS materials subjected to different post-cold-forming processes.

in RHS with different production histories. In particular, compression members made with RHS with large overall cross-sectional residual stresses are likely to experience early yielding, which in return leads to a reduction in stiffness and in turn a loss in load-carrying capacity.

As shown by the results in Figs. 17 and 18 as well as Table 7, the membrane components can be compressive or tensile depending on the location of measurement. For the bending components, all strips from all test pieces curved outward after sectioning, indicating compressive stresses on the inner surface of the RHS and tensile on the outer surface. The maximum residual stresses in general occur in the near corner regions. Similar observations have been made in the relevant research in the past [15,24,26,27]. Since the bending components (σ_b) are in general significantly larger than the membrane components (σ_m), the following discussions will focus on the former.

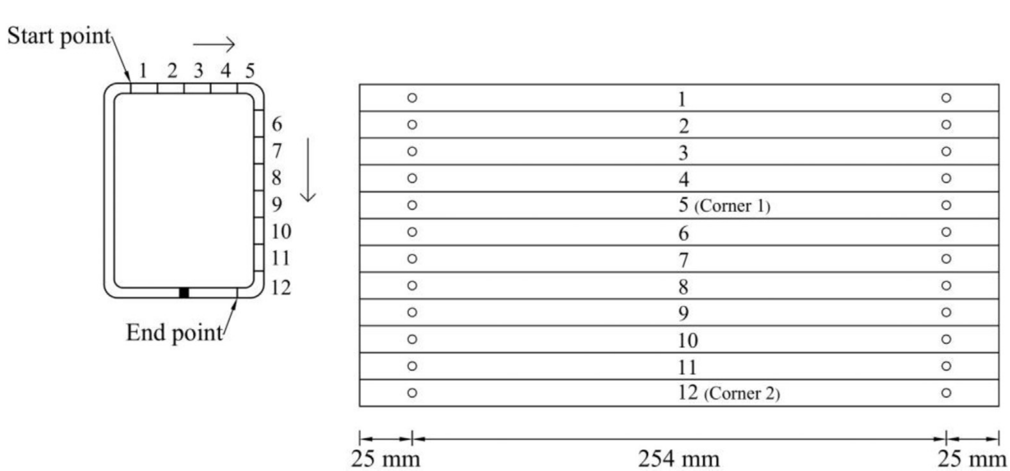

Fig. 12. Arrangement of strips around a typical RHS specimen (D-76 × 102 × 4.8-U).

Fig. 13. RHS specimen during sectioning.

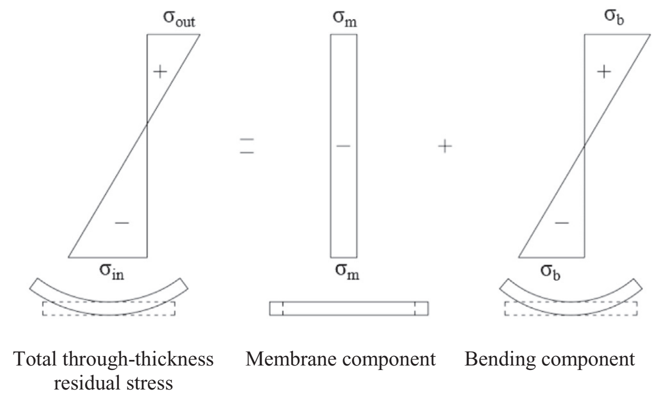

Fig. 16. Bending and membrane residual stress components.

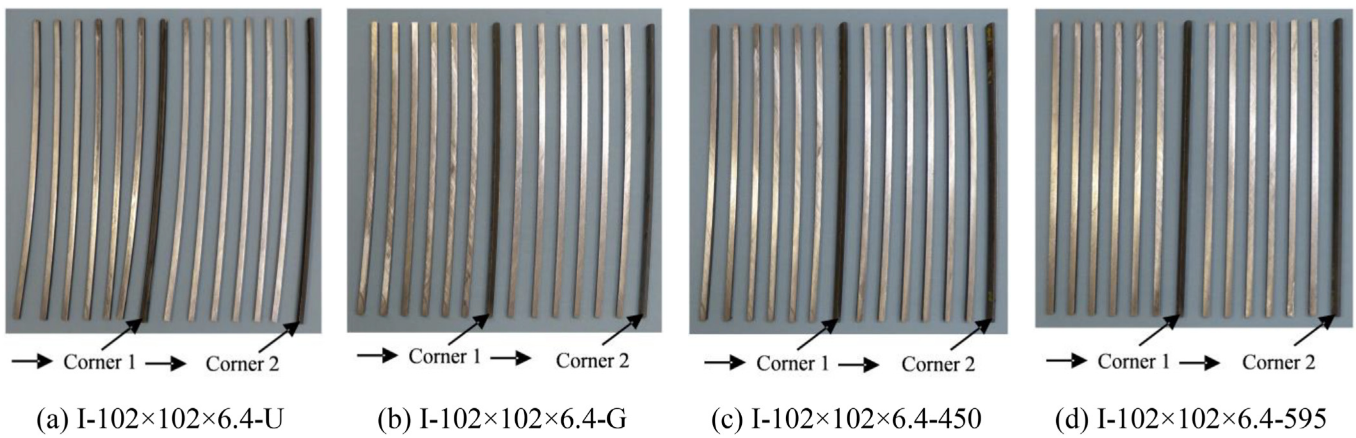

Fig. 14. Deformed strips from indirect-formed RHS subject to different post-cold-forming processes.

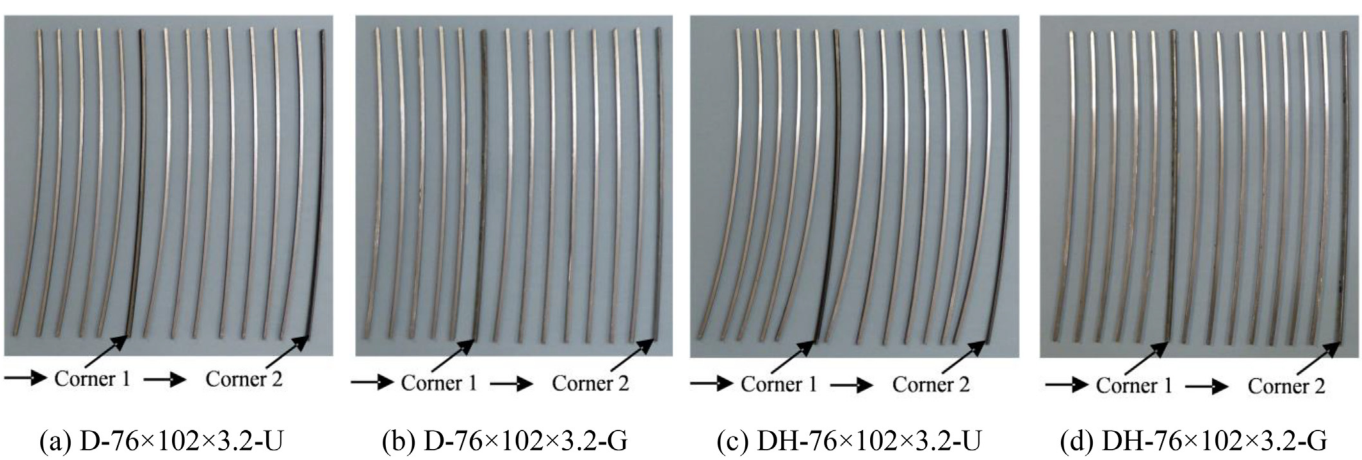

Fig. 15. Deformed strips from untreated and galvanized direct-formed RHS.

5.3. Discussions of residual stress measurement results.

5.3.1. Effects of cold-forming methods

As discussed in Section 3.1, the selection of the RHS specimens allows direct comparisons of residual stresses in untreated RHS cold-formed using different methods and coil materials of different grades. For each of the three groups (i.e. untreated direct-formed regular-strength RHS (D-U), untreated direct-formed high-strength RHS (DH-U), and untreated indirect-formed regular-strength RHS (I—U)), the average values of the overall cross-sectional bending residual stresses are calculated and listed in Table 7. The values are $0.66\sigma_y$, $0.56\sigma_y$ and $0.85\sigma_y$, respectively. It can be seen that the direct-forming

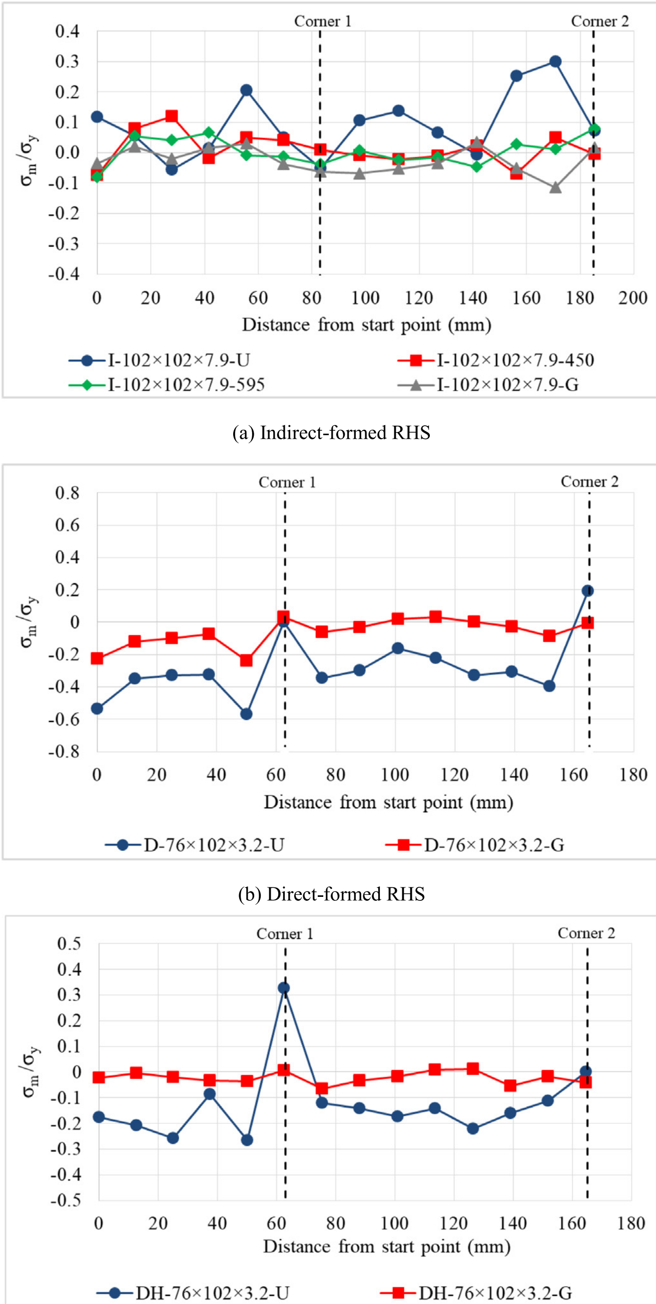

(a) Indirect-formed RHS

(b) Direct-formed RHS

(c) Direct-formed high-strength RHS

Fig. 17. Typical membrane residual stress distributions in RHS specimens.

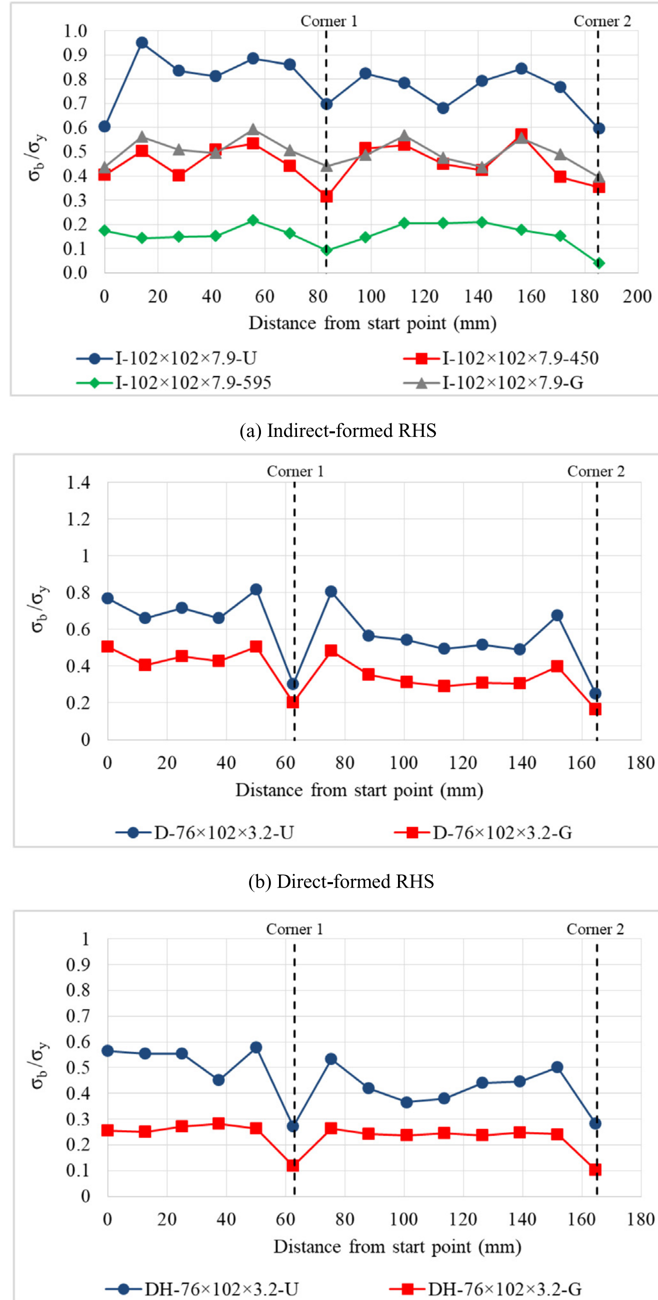

(a) Indirect-formed RHS

(b) Direct-formed RHS

(c) Direct-formed high-strength RHS

Fig. 18. Typical bending residual stress distributions in RHS specimens.

approach introduces a much lower level of residual stresses in the final RHS product, comparing to the indirect-forming approach. In particular, since the residual stress is a function of the cold-bending curvature rather than the strength of the coil material, the direct-formed high-strength RHS contains the lowest level of residual stress of all. This is consistent with its superior stub column behaviour reported by Tayyebi and Sun [6].

5.3.2. Effects of galvanizing and heat treatment

For the groups of galvanized direct-formed regular-strength RHS (D-G), galvanized high-strength direct-formed RHS (DH-G), and galvanized indirect-formed regular-strength RHS (I-G), the average values of the overall cross-sectional bending residual stresses are calculated and listed in Table 7. The values are $0.36\sigma_y$, $0.31\sigma_y$ and $0.48\sigma_y$, respectively. By comparing the values to those discussed in Section 5.2, it can be seen that the 10-min hot-dipping process is already very efficient in lowering the residual stresses. For the indirect-formed regular-strength RHS specimens heat treated to 450 °C (I-450) according to ASTM A1085 [7] or CSA G40.20/G40.21 [8] for a holding time of 30 min, the average value of the overall cross-sectional bending residual stresses is $0.46\sigma_y$, which is similar to the average value of the galvanized counterparts. This is consistent with results of the experimental research on galvanized and heat-treated RHS stub columns reported by Tayyebi and Sun [6]. Hence, one can speculate that the 30-min holding time used in the current industrial practice is excessively long. It should be noted that the aim of the ASTM A1085 [7] and the CSA G40.20/G40.21 [8] heat treatment is to provide a partial relief of residual stress

Table 7
Averages of normalized residual stresses in RHS specimens.

Specimen ID	Flat		Corner		Overall	
	σ_b/σ_y (%)	σ_m/σ_y (%)	σ_b/σ_y (%)	σ_m/σ_y (%)	σ_b/σ_y (%)	σ_m/σ_y (%)
I-102 × 102 × 6.4-U	82	-7	67	−2	80	−6
I − 102 × 102 × 6.4–450	41	-1	24	3	39	0
I-102 × 102 × 6.4–595	13	−4	5	−3	12	−4
I-102 × 102 × 6.4-G	45	2	37	−3	44	2
I-102 × 102 × 7.9-U	80	10	65	1	78	9
I-102 × 102 × 7.9–450	47	1	33	0	45	1
I-102 × 102 × 7.9–595	17	0	7	2	16	0
I-102 × 102 × 7.9-G	51	−3	42	−2	50	−3
I-102 × 102 × 13-U	99	1	87	10	97	2
I-102 × 102 × 13–450	58	2	37	11	55	3
I-102 × 102 × 13–595	11	−2	7	−1	10	−2
I-102 × 102 × 13-G	49	−2	52	−14	49	−4
D-76 × 102 × 3.2-U	64	−35	45	16	62	−27
D-76 × 102 × 3.2-G	40	−8	27	2	38	−6
D-76 × 102 × 4.8-U	62	−6	29	11	56	−3
D-76 × 102 × 4.8-G	37	−10	12	3	33	−8
D-102 × 102 × 4.8-U	88	−9	40	8	81	−7
DH-76 × 76 × 4.8-U	77	−5	35	11	69	−2
DH-76 × 76 × 4.8-G	41	−12	18	0	37	−10
DH-76 × 102 × 3.2-U	48	−17	33	19	46	−12
DH-76 × 102 × 3.2-G	25	−2	13	−2	24	−2
DH-76 × 102 × 4.1-U	54	−4	24	12	49	−2
DH-76 × 102 × 4.8-U	76	0	24	2	67	0
DH-76 × 102 × 4.8-G	37	−2	18	−3	34	−2
DH-76 × 152 × 4.1-U	52	−9	25	7	49	−7
DH-76 × 152 × 4.1-G	30	−10	10	6	27	−8
Average D-U	71	−17	38	12	66	−12
Average D-G	39	−9	20	3	36	−7
Average DH-U	61	−7	28	10	56	−5
Average DH-G	33	−7	15	0	31	−6
Average I-U	87	1	73	3	85	2
Average I-G	48	−1	44	−6	48	−2
Average I-450	49	1	31	5	46	1
Average I-595	14	−2	6	−1	13	−2

throughout the cross section for better compressive member behaviour. In Canada, such heat treatment justifies the use of a higher column curve in the steel design standard CSA S16–19 [12]. According to the experimental findings of this research, a 10-min holding time for a heat treatment at 450 °C serves the purpose already. Hence, the current industrial practice for such heat treatment needs to be revisited. On the other hand, for the indirect-formed regular-strength RHS specimens heat treated to 595 °C (I-595) according to ASTM A143 [14], the average value of the overall cross-sectional bending residual stresses is only $0.13\sigma_y$. However, when specifying such heat treatment, the trade-off among residual stress, material ductility and strength must be taken into consideration by the designers and fabricators.

6. Conclusions

This paper reports the tensile coupon test results of 26 rectangular hollow section (RHS) specimens with different grades (nominal yield strengths from 350 to 690 MPa), produced by different cold-forming techniques (indirect-forming versus direct-forming), and subjected to various post-production heat-treatment and galvanizing processes. Using the sectioning method, a total of 342 strips were carefully machined from the 26 RHS specimens for a comprehensive residual stress measurement.

Based on the residual stress data presented in this paper, and the column test results reported by Tayyebi and Sun [6] as well as Shi et al. [4,5], it can be concluded that the current North American industrial practice for hot-dip galvanizing can effectively reduce the residual stress level in cold-formed HSS (rectangular and circular), similar to a heat treatment process described in ASTM A1085 Supplement S1 [7], and CSA G40.20/G40.21 [8]. This in turn can improve the column behaviour. The holding time of 30 min used in the current industrial practice for heat treatment to an ASTM A1085 [7] or CSA G40.20/G40.21 [8] finish may be excessively long. A holding time of 10 min for such heat treatment may be sufficient already.

The direct-forming approach introduces a much lower level of residual stresses in the final RHS product, comparing to the indirect-forming approach. In addition, since the residual stress is primarily a function of the cold-bending curvature rather than the strength of the coil material, the direct-formed high-strength RHS contains the lowest level of normalized residual stress.

Symbols

B	Measured width
D	Chord length
E	Young's modulus
H	Measured depth
r_i	Inner corner radius
t	Measured thickness
ε	Measured strain
ε_r	Rupture strain of coupons
ε_u	Strain at ultimate stress of coupons
σ_b	Bending residual stress
σ_{in}	Total residual stress on inner surface of RHS in longitudinal direction
σ_m	Membrane residual stress
σ_{out}	Total residual stress on outer surface of RHS in longitudinal direction
σ_u	Measured ultimate stress
σ_y	Measured yield stress
$\sigma_{y,nom}$	Nominal yield stress

Acronyms

CE	Carbon Equivalent value
HSS	Hollow structural section
RHS	Rectangular hollow section

Author statement

The work has not been published previously. It is not under consideration for publication elsewhere. The publication is approved by all authors. If accepted, it will not be published elsewhere in the same form, in English or in any other language, including electronically without the written consent of the copyright-holder.

Declaration of Competing Interest

The authors declare that they have no known competing financial interests or personal relationships that could have appeared to influence the work reported in this paper.

Acknowledgements

The authors are grateful for the financial support from the Canadian Institute of Steel Construction (CISC), the British Columbia Institute of Technology (BCIT), and the Natural Sciences and Engineering Research Council of Canada (NSERC). Silver City Galvanizing, Bull Moose Tube, McAllister Industries, and Park Derochie have donated materials and services to support this research.

References

[1] J.A. Packer, S.P. Chiew, R. Tremblay, G. Martinez-Saucedo, Effect of material properties on hollow section performance, Proc. Inst. Civ. Eng. - Struct. Build. 163 (2010) 375–390.
[2] M. Sun, J.A. Packer, Hot-dip galvanizing of cold-formed steel hollow sections: a state-of-the-art review, Front. Struct. Civ. Eng. 13 (2019) 49–65.
[3] M. Sun, Z. Ma, Effects of heat-treatment and hot-dip galvanizing on mechanical properties of RHS, J. Constr. Steel Res. 153 (2019) 603–617.
[4] G. Shi, X. Jiang, W. Zhou, Y. Zhang, Experimental study on overall buckling behavior of Q420 high strength welded galvanized tubes under axial compression, J. Harbin Inst. Technol. 45 (2013) 75–80.
[5] G. Shi, X. Jiang, W. Zhou, T.-M. Chan, Y. Zhang, Experimental investigation and modeling on residual stress of welded steel circular tubes, Int. J. Steel Struct. 13 (2013) 495–508.
[6] K. Tayyebi, M. Sun, Stub column behaviour of heat-treated and galvanized RHS manufactured by different methods, J. Constr. Steel Res. 166 (2020) 105910.
[7] ASTM, Standard Specification for Cold-Formed Welded Carbon Steel Hollow Structural Sections (HSS), ASTM A1085/A1085M-15, American Society for Testing and Materials, West Conshohocken, PA, USA, 2015.
[8] CSA, General requirements for rolled or welded structural quality steel / Structural quality steel, CSA G40.20–13/G40.21–13, Canadian Standards Association, Toronto, Canada, 2013.
[9] M.A. Serrano-López, C. López-Colina, J.J. del Coz-Díaz, F.L. Gayarre, Static behavior of compressed braces in RHS K-joints of hot-dip galvanized trusses, J. Constr. Steel Res. 89 (2013) 307–316.
[10] S. Daneshvar, M. Sun, K. Karimi, Galvanized RHS X-connections. I: effects of vent and drain holes on SCFs, J. Constr. Steel Res. (2019) 105854.
[11] S. Daneshvar, M. Sun, Stress concentration factors of RHS T-connections with galvanizing holes under in-plane bending, J. Constr. Steel Res. 169 (2020) 106039.
[12] CSA, Limit States Design in Structural Steel, CSA S16–19, Canadian Standard Association, Toronto, ON, Canada, 2019.
[13] M. Sun, J.A. Packer, Charpy V-notch impact toughness of cold-formed rectangular hollow sections, J. Constr. Steel Res. 97 (2014) 114–126.
[14] ASTM, Standard Practice for Safeguarding against Embrittlement of Hot-Dip Galvanized Structural Steel Products and Procedure for Detecting Embrittlement, ASTM A143/A143M-07, American Society for Testing and Materials, West Conshohocken, PA, USA, 2014.
[15] S.H. Li, G. Zeng, Y.F. Ma, Y.J. Guo, X.M. Lai, Residual stresses in roll-formed square hollow sections, Thin-Walled Struct. 47 (2009) 505–513.
[16] L. Tong, G. Hou, Y. Chen, F. Zhou, K. Shen, A. Yang, Experimental investigation on longitudinal residual stresses for cold-formed thick-walled square hollow sections, J. Constr. Steel Res. 73 (2012) 105–116.
[17] J.L. Ma, T.M. Chan, B. Young, Experimental investigation of cold-formed high strength steel tubular beams, Eng. Struct. 126 (2016) 200–209.
[18] T.M. Chan, X.L. Zhao, B. Young, Cross-section classification for cold-formed and built-up high strength carbon and stainless steel tubes under compression, J. Constr. Steel Res. 106 (2015) 289–295.
[19] J.L. Ma, T.M. Chan, B. Young, Design of cold-formed high strength steel tubular beams, Eng. Struct. 151 (2017) 432–443.
[20] J.L. Ma, T.M. Chan, B. Young, Design of cold-formed high-strength steel tubular stub columns, J. Struct. Eng. 144 (2018), 04018063.
[21] X. Lan, J. Chen, T.M. Chan, B. Young, The continuous strength method for the design of high strength steel tubular sections in compression, Eng. Struct. 162 (2018) 177–187.
[22] X. Lan, J. Chen, T.M. Chan, B. Young, The continuous strength method for the design of high strength steel tubular sections in bending, J. Constr. Steel Res. 160 (2019) 499–509.
[23] L. Gardner, N. Saari, F. Wang, Comparative experimental study of hot-rolled and cold-formed rectangular hollow sections, Thin-Walled Struct. 48 (2010) 495–507.
[24] M. Sun, J.A. Packer, Direct-formed and continuous-formed rectangular hollow sections — comparison of static properties, J. Constr. Steel Res. 92 (2014) 67–78.
[25] M. Sun, J.A. Packer, High strain rate behaviour of cold-formed rectangular hollow sections, Eng. Struct. 62–63 (2014) 181–192.
[26] J.L. Ma, T.M. Chan, B. Young, Material properties and residual stresses of cold-formed high strength steel hollow sections, J. Constr. Steel Res. 109 (2015) 152–165.
[27] B. Somodi, B. Kövesdi, Residual stress measurements on cold-formed HSS hollow section columns, J. Constr. Steel Res. 128 (2017) 706–720.
[28] J.L. Ma, T.M. Chan, B. Young, Experimental investigation on stub-column behavior of cold-formed high-strength steel tubular sections, J. Struct. Eng. (United States) 142 (2016) 04015174.
[29] J. Wang, S. Afshan, N. Schillo, M. Theofanous, M. Feldmann, L. Gardner, Material properties and compressive local buckling response of high strength steel square and rectangular hollow sections, Eng. Struct. 130 (2017) 297–315.
[30] B. Somodi, B. Kövesdi, Flexural buckling resistance of cold-formed HSS hollow section members, J. Constr. Steel Res. 128 (2017) 179–192.
[31] B. Young, W.M. Lui, Behavior of cold-formed high strength stainless steel sections, J. Struct. Eng. 131 (11) (2005) 1738–1745.
[32] Y. Huang, B. Young, Material properties of cold-formed lean duplex stainless steel sections, Thin-Walled Struct. 54 (2012) 72–81.
[33] Y. Huang, B. Young, The art of coupon tests, J. Constr. Steel Res. 96 (2014) 159–175.
[34] ASTM, Standard Specification for Cold-Formed Welded High Strength Carbon Steel or High-Strength Low-Alloy Steel Hollow Structural Sections (HSS) in Rounds and Shapes, ASTM A1112/A1112M - 18, American Society for Testing and Materials, West Conshohocken, PA, USA, 2018.
[35] ASTM, Tension Testing of Metallic Materials, ASTM E8/E8M-16a, American Society for Testing and Materials, West Conshohocken, PA, USA, 2016.
[36] CEN, Eurocode 3—Design of Steel Structures—Part 1–1: General Rules and Rules for Buildings, BS EN-1993-1-1, British Standards Institution, London, UK, 2005.
[37] CEN, Eurocode 3—Design of Steel Structures—Part 1–12: Additional Rules for the Extension of EN 1993 Up to Steel Grades S 700, BS EN-1993-1-1, British Standards Institution, London, UK, 2007.
[38] ANSI/AISC, Specification for Structural Steel Buildings, ANSI/AISC 360–10, Chicago, IL, USA, 2016.
[39] ASTM, Standard Specification for Cold-Formed Welded and Seamless Carbon Steel Structural Tubing in Rounds and Shapes, ASTM A500/A500M - 18, American Society for Testing and Materials, West Conshohocken, PA, USA, 2018.
[40] R.D. Ziemian, Guide to Stability Design Criteria for Metal Structures, John Wiley & Sons, Hoboken, USA, 2010.
[41] Y.B. Wang, G.Q. Li, S.W. Chen, The assessment of residual stresses in welded high strength steel box sections, J. Constr. Steel Res. 76 (2012) 93–99.
[42] H.X. Yuan, Y.Q. Wang, Y.J. Shi, L. Gardner, Residual stress distributions in welded stainless steel sections, Thin-Walled Struct. 79 (2014) 38–51.
[43] G.W. Li, Y.Q. Li, J. Xu, X. Cao, Experimental investigation on the longitudinal residual stress of cold-formed thick-walled SHS and RHS steel tubes, Thin-Walled Struct. 138 (2019) 473–484.
[44] R.B. Cruise, L. Gardner, Residual stress analysis of structural stainless steel sections, J. Constr. Steel Res. 64 (3) (2008) 352–366.